2013 IEEE/RSJ International Conference on
Intelligent Robots and Systems (IROS)
November 3-7, 2013. Tokyo, Japan

Multi-Joint Gripper with Stiffness Adjuster

T. Tamamoto and K. Koganezawa

Abstract—**This paper proposes a multi-joint-gripper that achieves envelope grasping for unknown shape objects. Proposed mechanism is based on a chain of Gear Systems controlled by only one motor. It also has a Variable Stiffness Mechanism (VSM) that controls joint stiffness to relieve interfering effects suffered from grasping environment and achieve a dexterous grasping. The experiments elucidate that the developed gripper achieves envelop grasping; the posture of the gripper automatically fits the shape of the object with no sensory feedback. And they also show that the VSM effectively works to relieve external interfering. This paper shows the detail of the mechanism and the experiments of its motion.**

Keywords-envelope grasping; multi-joint-gripper; variable-stiffness;

I. INTRODUCTION

The fatal disaster of the Fukushima nuclear plant being brought about by the earthquake and subsequently assaulting tsunami on March 11 in 2011 revealed the disability of the current robot technology when it faced with such disastrous environments. It also prompts to develop a new type of autonomous robot that should have tough and effective hand or gripper. The forthcoming robots used in an ultimate environment should satisfy the following requirements.

Back-drivability (BD): End-effectors always interact with external environment, of which effect should not be expected to be predictable. This fact requires the end-effecter to have some "resiliency" to external interaction, which is interpreted as "back-drivability" of the joints in the technical point of view.

Inherently safe design (ISD): This property is much related to the BD in the sense that the end-effecter is never harmful to external environment (especially to human). In addition to the BD, ISD requires some items as follows.

(a) Any electric/electronic devices or sensors should not be equipped on the portions that directly contact with external objects. Since the robots have to cope with expected severe environments, such as electromagnetic or radio-active fields.

(b) According to (a) the controller cannot much rely on the feedback from sensors such as tactile or pressure sensors.

ISD does not completely deny using sensory feedback, which might be helpful to accomplish some dexterous and precise motion of the end-effector if a measure against radio active noise is satisfactory. Therefore ISD requires that some primitive motions of the end-effecter should be provided without sensory feedback, in other words, mechanically, but it allows using the sensory feedback as subsidiary measures.

Simple Control (SC): The control should be as simple as possible. This requirement will be achieved along with pursuing the above BD and ISD requirements. BD will reduce the control burden to determine the end-effector's motion when they interact with external objects. ISD also provides a simple control that does not much rely on the sensory feedback.

But most of all, the SC requirement prompts us to reduce the end-effector's DOF as far as possible.

In this paper, we propose a multi-joint gripper that achieves envelope grasping for unknown-shape object under fulfilling the BD, ISD and SC requirements described above.

The pioneering work in this field will be the "soft gripper" developed by Hirose and Umetani[1]. The wire driven series of joint became the most typical mechanical architecture that has been followed by a lot of subsequent studies[2-6]. The mechanisms proposed in these studies will satisfy the BD, ISD and SC requirements or a part of them, but the most crucial problem of these studies resides in using much number of wires for driving series of joints, which gives rise to the following troubles on actual assembling and controlling.

(a) Elasticity of the wire combined with the friction with pulleys sometimes causes unpredictable vibratory behavior of the gripper.

(b) There exists singular posture of the gripper, especially of those having much number of serial joints.

(c) Binding wires with appropriate tension is much cumbersome than one imagines and the tension is temperature dependent.

So this paper proposes a novel mechanism without using wire on its power transmission parts. We also propose a mechanism of adjusting stiffness of joints, which allows the gripper to vary the joint stiffness according to interactive conditions with grasping objects.

This paper is organized as follow. In the following section it shows a mechanism of the proposed gripper, the principle of its motion and shape-fitting property to show it having the back-drivability. In the third section it shows the variable stiffness mechanism (VSM) equipped in the gripper to achieve dexterous grasping. The forth section is devoted to the simulation study. In fifth section the constructed test machine is introduced and some motion tests are shown. The last section is devoted to some conclusive remarks.

Manuscript received March 4, 2013.

T. Tamamoto and K. Koganezawa are with the Dep. of Mechanical Engineering, Tokai University, 4-1-1 Kitakaname Hiratsuka, Kanagawa 259-1292 Japan
(phone +81-463-58-1211; fax: +81-463-59-2207;
e-mail; kogane@keyaki.cc.u-tokai.ac.jp)

II. DRIVE MECHANISM

A. Active/Passive amalgamation

We consider a planar multi-joint gripper of which driving torque is generated by only one motor and is transmitted to a distal end of the gripper via serially connected rotary joints. Fig.1 shows the outline of the driving mechanism of the proposed gripper. Fig.1(b) shows the differential gear system used as a core component. The system is a 2 input 1 output system. One of the input torque is given to the gear A. The gear C is the output of which rotation is transmitted to the next unit. Every joint has this transmission system and they are serially connected by timing belts and pulleys as shown in Fig.1(c). The rotation of the motor is transmitted to the pulley-A that is located at the first joint by a timing belt. Then, the rotation is transmitted to the next pulley-A via the following pulley-belt chain. Pulley-B (B1, B2) interlock with the middle shaft. If the middle shaft is rotated relative to link, a back torque generated by the stopper mechanism (detail is explained in the next section) works to hamper the rotation. On the other hand, the link rotation caused by external force or torque brings about the rotation of the pulley-B, and also that of the next pulley-A.

The mechanism, therefore, allows an amalgamation of the two inputs; one is an active torque input into the pulley-A and the other is a passive torque input into the pulley-B of which stiffness is controlled by the stopper mechanism as explained in the next section. The beneficial points of this mechanism are as follows:

1) Each joint is uncoupled with respect to torque transmission. By contrast, some mechanisms proposed in the past studies are coupled because all of the joints are remotely controlled from the base by using elongated wires[1][2] , which will sometimes cause the gripper to take irreversible singular postures.

2) Almost all elasticity elements of the system concentrates on springs as explained later, although the elasticity of timing belts exist but can be negligible. Moreover, the passive torque due to springs and the active torque due to the motor are separated. These facts make kinetic and dynamic analysis of the system very simple.

B. Envelope grasping

If there is no disturbance, the relative angle of the i'th link θ_{Li} is determined as,

$$\theta_{Li} = \theta_{Ai} \tag{1}$$

where θ_{Ai} is rotation angles of the i'th pulley-A. And transmission of rotation from pulley-A to the next pulley-A is determined as,

$$\theta_{Ai+1} = \left\{\frac{D_2(B_1C - AB_2)}{B_1D_1E} - 1\right\}\theta_{Li} + \frac{AB_2D_2}{B_1D_1E}\theta_{Ai} \tag{2}$$

where "A" to "E" are the teeth numbers of each pulley. Here in accordance with Fig.1, we only use two teeth numbers. Denoting Zl and Zs as teeth numbers of the large and small pulleys respectively, Eq.(2) is simplified as,

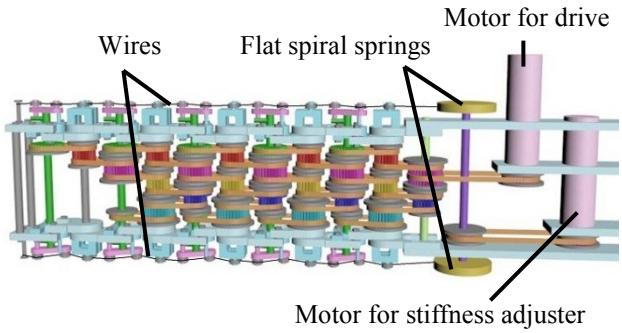

(a) Overall view of the 5 joints gripper

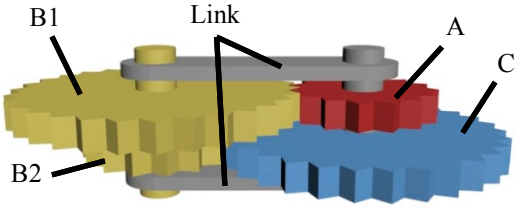

(b) Differential Gear System

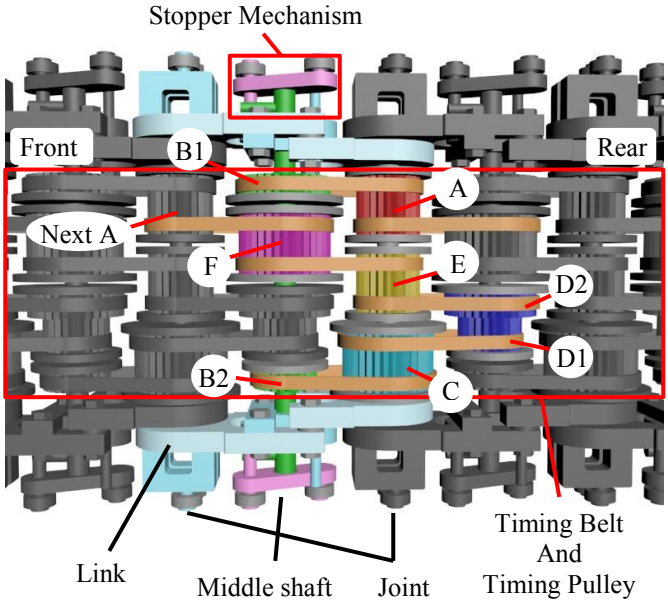

(c) Pulley train of one unit

Fig.1 Drive mechanism

$$\theta_{Ai+1} = \left(\frac{Zl^2 - Zs^2}{Zs^2} - 1\right)\theta_{Li} + \theta_{Ai} \tag{3}$$

Setting Zl=17 and Zs =12, a uniform transmission of rotation can be achieved as follows.

$$\theta_{Ai+1} = \frac{1}{144}\theta_{Li} + \theta_{Ai} \approx \theta_{Ai} \tag{4}$$

Eq(4) suggests the rotation angle of the (i+1)th pulley is determined by that of the previous one almost irrespective of the link rotation. Thus the rotation is transmitted to the distal end, even if one link is hampered to rotate by the object (Fig.2).

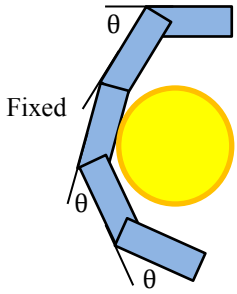

Fig.2 Mechanism of envelope grasping

III. VARIABLE STIFFNESS MECHANISM (VSM)

A. Stopper mechanism

The stopper mechanism is for generating a back torque when the middle shaft is rotated relative to the link. Fig.3 shows the outline of the Stopper mechanism. The wire is connected to one end of the flat spiral spring (FSS, hereafter) and link of fingertips (see Fig.1). The FSS generates the wire tension, which is controlled by another motor (the "motor for stiffness adjuster" in Fig.1). This mechanism is equipped on upper and lower sides of the link but controlled by the same motor. Their motion is limited to clockwise and counterclockwise rotations respectively. Fig.3 is a counterclockwise case, in which clockwise torque works on the stopper plate by the wire tension. And the stopper-A transmits a back torque when the middle shaft is rotated counterclockwise. If the middle shaft is rotated clockwise, the stopper plate does not rotate with no loosening of the wire due to the stopper-B. The wires are smoothly pulled or loosened with ball bearings. Due to installing the stopper mechanisms in the upper and the lower sides that work for opposite directions, the gripper can move in both directions.

Setting $\theta_{Ai+1} = \theta_{Ai}$ according to Eq.4, the angle of middle shafts "δ_i" is determined as:

$$\delta_i = \frac{Zs}{Zl}(\theta_{Ai} - \theta_{Li}) = \frac{12}{17}(\theta_{Ai} - \theta_{Li}) \qquad (5)$$

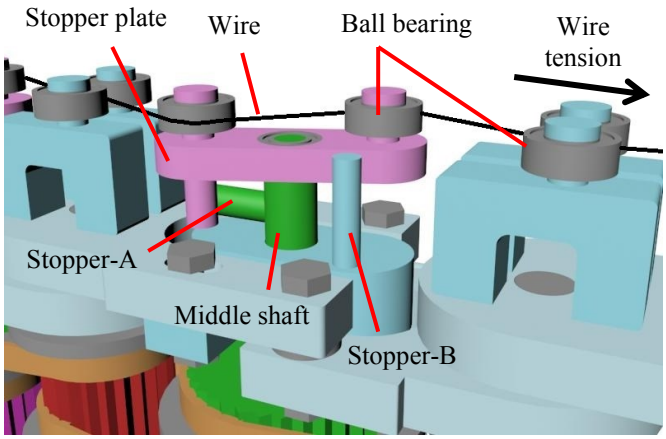

Fig.3 Stopper mechanism

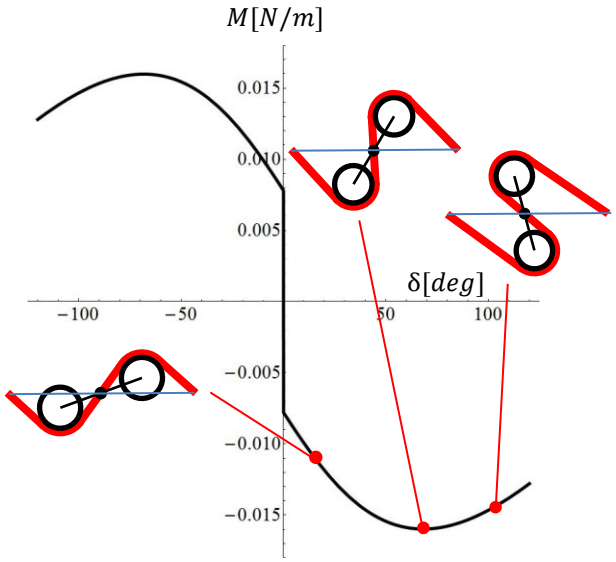

Fig.4 Characteristics of the back torque

Fig.4 shows the relationship between the angle of middle shaft and the back torque "M (δ_i)"(when wire tension=1 N). Due to the configuration of the stopper mechanism, $M(0)$ has some non-zero value that is determined by the wire tension. It is crucial because if it allows $M(0)=0$, ith joint becomes in a free rotating state when $\delta_i = 0$ irrespective of the wire tension, which causes an unstable state against external disturbances.

B. VSM

The *soft gripper*'s motion is affected by external force or torque including its own weight, inertia forces or another coupling force or torque. Therefore relatively high-stiffness is desirable under no contact with objects to assure almost precise synergic flexion. Once the gripper contacts objects and starts the envelope grasping, it should adjust its stiffness according to the object's elasticity. To fulfill the requirement we develop the variable stiffness mechanism (VSM) and employ it into the gripper.

One end of the flat spiral spring is connected to the shaft (see Fig.1) that is rotated by a motor to adjust the wire tension. According to the stopper mechanism, the wire tension determines the stiffness of the middle shaft.

IV. SIMULATION

In order to check the motion of the gripper and to seek the way to control, the dynamic simulation is performed (Five joints model). The equations of motion are derived based on Lagrange's method:

$$\frac{d}{dt}\left(\frac{\partial L}{\partial \dot{q}}\right) - \frac{\partial L}{\partial q} + \frac{\partial V}{\partial \dot{q}} = Q \qquad (6)$$

where "L" is Lagrangian, "V" is dissipation energy. "Q" is external torques. Generalized coordinates "q" is a vector including the angle of the motor for drive, the relative angles of each links and coordinate of object (see Fig.5).

$$q = \left[\theta_M\ \theta_1\ \theta_2\ \theta_3\ \theta_4\ \theta_5\ G_x\ G_y\ G_\theta\right]^T \qquad (7)$$

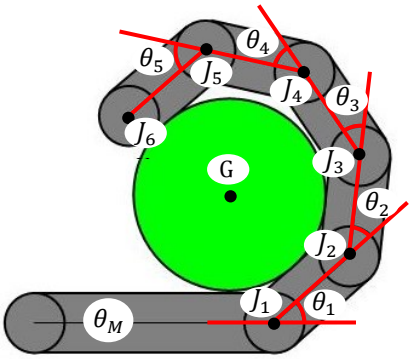

Fig.5 Five joints simulation model

Dissipation energy depends on the speeds "$\dot{q}$". Kinetic energy is the force of inertia of each link and object. The potential energy due to the gravity is ignored because of assuming horizontal motion. Torque by the motor and wire is treated as an external force. External force Q and motor torque Q_m are determined as:

$$Q = Q_m + Q_k + Q_R \tag{8}$$

$$Q_m = [P_d\ 0\ 0\ 0\ 0\ 0\ 0\ 0\ 0] \tag{9}$$

where P_d represents a PD control input using the target angle and the current angle of the motor. Q_k is the back torque acting on the middle shaft. Using the principle of virtual work, the torque acting on the each joint Q_j and their class vector Q_k are determined as:

$$Q_j = \begin{bmatrix} \frac{\partial \delta_1}{\partial \theta_1} & \cdots & \frac{\partial \delta_5}{\partial \theta_1} \\ \vdots & \ddots & \vdots \\ \frac{\partial \delta_1}{\partial \theta_5} & \cdots & \frac{\partial \delta_5}{\partial \theta_5} \end{bmatrix} \begin{bmatrix} M(\delta_1) \\ \vdots \\ M(\delta_5) \end{bmatrix} \tag{10}$$

$$Q_k = \left[0\ Q_{j_1}\ Q_{j_2}\ Q_{j_3}\ Q_{j_4}\ Q_{j_5}\ 0\ 0\ 0\right]^T \tag{11}$$

Q_R is an external torque caused by the contact with object. Detail is described below. By solving Eq.6, the each link angle is determined. Joint positions are simply determined as:

$$J_{i+1} = \begin{bmatrix} Jx_{i+1} \\ Jy_{i+1} \end{bmatrix} = \begin{bmatrix} Jx_i \\ Jy_i \end{bmatrix} + l \begin{bmatrix} \cos\theta_i \\ \sin\theta_i \end{bmatrix} \tag{12}$$

assuming a constant link length l. The penalty method that treats objects as elastic bodies is used for dealing with contact. Contact of the object and the link is determined as (see Fig.6):

$$x \le r + w/2 \tag{13}$$

$$0 \le lx \le l \tag{14}$$

If this equation is satisfied the link and object are in contact. At this time, the reaction force R is determined as:

$$R = k \cdot \left(x - r - \frac{w}{2}\right) \begin{bmatrix} -Jy_{i+1} + Jy_i \\ Jx_{i+1} - Jx_i \end{bmatrix} / l \tag{15}$$

where R is a vector in the direction perpendicular to the link i. The position of the contact points are calculated in two ways: one is from the link coordinate $P[\theta_1, \cdots, \theta_5]$ and the other is from the object coordinate $P'[G_x\ G_y\ G_\theta]$. Then the external

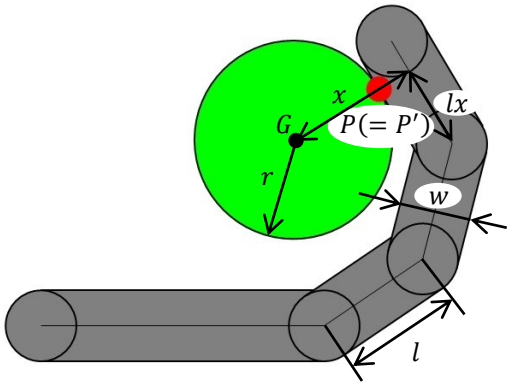

Fig.6 Contact with cylinder

torque T acting on the each joint, that of acting on the object F by reaction force and their class vector Q_R are calculated by:

$$T = \begin{bmatrix} \sum_{k=1}^{5} \frac{\partial P_x}{\partial \theta_k} & \sum_{k=1}^{5} \frac{\partial P_y}{\partial \theta_k} \\ \vdots & \vdots \\ \sum_{k=5}^{5} \frac{\partial P_x}{\partial \theta_k} & \sum_{k=5}^{5} \frac{\partial P_y}{\partial \theta_k} \end{bmatrix} \begin{bmatrix} R_x \\ R_y \end{bmatrix} \tag{16}$$

$$F = \begin{bmatrix} \frac{\partial P'_x}{\partial G_x} & \frac{\partial P'_y}{\partial G_x} \\ \frac{\partial P'_x}{\partial G_y} & \frac{\partial P'_y}{\partial G_y} \\ \frac{\partial P'_x}{\partial G_\theta} & \frac{\partial P'_y}{\partial G_\theta} \end{bmatrix} \begin{bmatrix} -R_x \\ -R_y \end{bmatrix} \tag{17}$$

$$Q_R = [0\ T_1\ T_2\ T_3\ T_4\ T_5\ F_1\ F_2\ F_3]^T \tag{18}$$

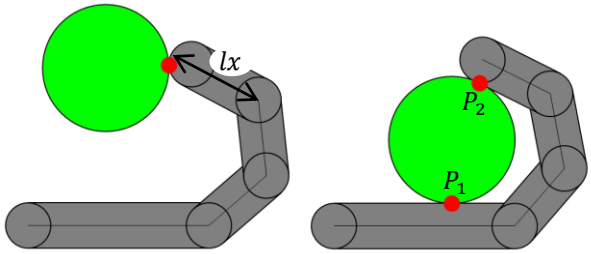

(a) tip contact (b) Plural contact

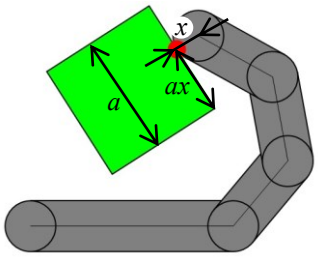

(c) Contact with square object

Fig.7 Contact with a variety

As a special case, there are some contact cases that not satisfy the equation (14). Fig.7(a) is the case of contacting at the tip. In this case, w is set as zero. In the case of existing more than one contact points as shown Fig.7(b), Q_R are calculated the number of times of the contact points.

In the case of square shape object, it is necessary to calculate the edge of the object and joint contact (see Fig.7). In this case, the contact of the object and the link is detected with:

$$x \leq w/2 \tag{19}$$

$$0 \leq ax \leq a \tag{20}$$

Table I shows the parameters used in the simulation. Elastic modulus of the objects is determined try and error so that the link is not affected undue rebounding at the moment of the contact.

Fig.8 shows the results of simulations, the cases of the circular and the square shape objects. The red arrows at the contact points show the reaction force vectors. As shown the reaction forces are well distributed in the plural contact case.

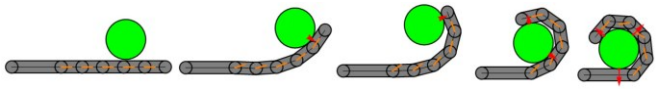

(a) Circular object grasping

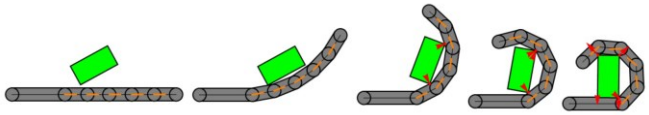

(b) Square object grasping

Fig.8 Two results of envelope grasping simulation

TABLE I. Simulation parameter	
Length between the joint [mm]	45
Height of the fingers [mm]	27
Weight of the one link [g]	140
Elastic modulus of object [N/ m^2]	300
Size of object [mm]	(a) Ø80 (b) 40 × 80
Weight of object [g]	100
Numerical calculation	Runge-Kutta method
Target angle of the motor [deg]	50

V. TEST MACHINES

We developed the test machine as shown in Fig.9. It has five joints. Table II shows physical parameters of the test machine.

TABLE II. Design parameter of the experimental machine

Length of the fingers [mm]	225
Length between the joint [mm]	45
Height of the fingers [mm]	27
Width of the fingers [mm]	100
Weight of the fingers [g]	730
Actuator	maxson EC22 × 2 Blushless 50W Gear 370:1

A. Envelope grasping

Fig.10 shows the envelope grasping of the machine with various shape objects. We observe that the machine achieved the well-balanced envelope grasping. It is noteworthy that all of the motions shown in Fig.10 are achieved by the identical PD control of the motor with no sensory feedback.

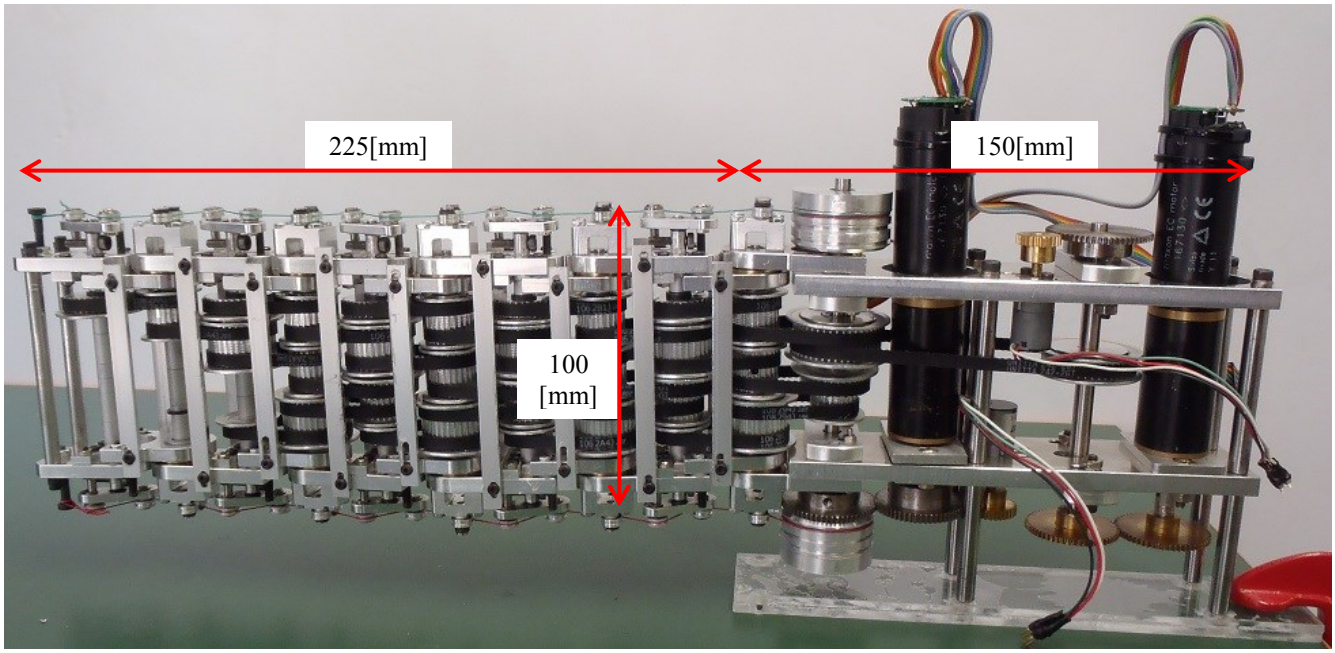

Fig.9 Appearance of the five joints test machine

B. Effect of the VSM

The effect of the VSM is evaluated by the following experiments. It is observed the difference of the grasping speed between the cases of high stiffness and low stiffness, even if the same rotation of the motor is given. Fig.11 shows a snapshot of every 0.5 seconds after the motor onset. This result indicates that the response of the link motion is delayed by an inertial force when the joints are in a low stiffness state and it is improved by augmenting the wire tension of the VSM; high stiffness state.

Fig.12 is an experiment in the case of gripping the soft object. At first the machine grips the paper cup in a low stiffness state, then switched in a high stiffness state. As shown the high stiffness brings about deforming soft objects.

From these two experiments, the optimum gripping operation is as follows. Before contact with the object, the gripper should be driven in a high stiffness state. After contact with the object, it should be driven in an appropriate low stiffness state.

VI. CONCLUSIONS

A novel mechanism of the multi-joint gripper is proposed and the test machine was developed. It allows the active/passive torque amalgamation with no torque coupling between the joints. The experiments of the test machines elucidated the proposed mechanism achieves one DOF synergic flexion and envelope grasping of various shape objects. The variable stiffness mechanism (VSM) is also proposed and implemented into the test machine. It is a mechanism decoupled with the driving parts of the gripper. Therefore the stiffness of the joints can be adjusted independently with the motor for stiffness adjuster. The experiments showed the VSM effectively improves the motion of the gripper. It can be concluded the proposed gripper satisfies the BD, ISC and SC requirements that are defined in the introduction.

We are now planning to construct the second machine, in which the height will be drastically shortened.

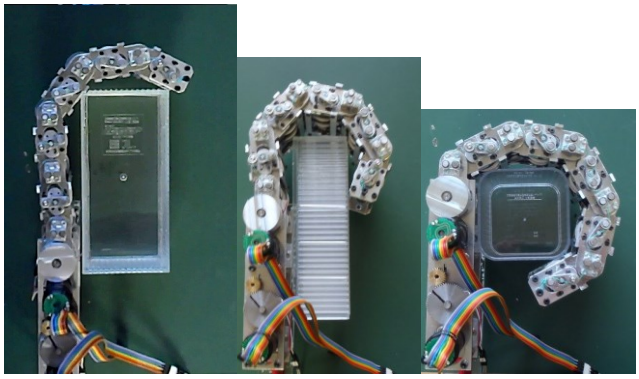

Fig.10 Envelope grasping of various shape objects

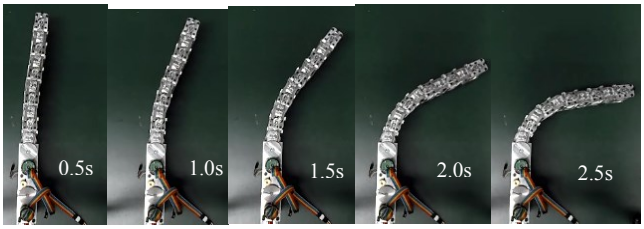

(a) Low Stiffness state

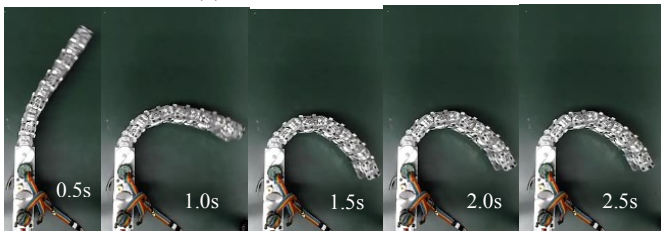

(b) High Stiffness state

Fig.11 Motion in different stiffness states

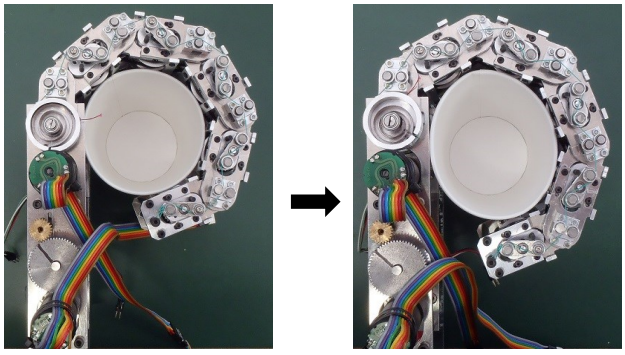

(a) Low Stiffness (b) High Stiffness

Fig.12 Envelope grasping of soft object

REFERENCES

[1] S. Hirose and Y. Umetani, "The Development of Soft Gripper for the Versatile Robot Hand," Mechanism and Machine Theory, Pergamon Press, 13, pp.351-359 (1978)

[2] S. Hirose and S. Ma, "Coupled tendon-driven multijoint manipulator," IEEE Intern. Conf.on Robotics and Automation, pp. 1268-1275, 1991.

[3] S. Hirose, "Biologically Inspired Robots (Snake-like Locomotor and Manipulator), " Oxford University Press , 1993.

[4] N. Dechev. W. L. Clegjhorn and S. Naumann, "Multiple Finger, Passive Adaptive Grasp Prosthesis Hand," Mechanism Machine Theory, Vol.36, No.10, pp.1157-1173, 2001.

[5] B. Massa, S. Roccella, M. C. Carrozza and P. Dario, "Design and Development of an Underactuated Prosthetic Hand," Proc. Of the 2002 IEEE Intern., Conf. on Robotics & Autom., pp.3374-3379, 2002.

[6] M. Wassink, R. Carloni and S. Stramigioli, "Port-Hamiltonian Analysis of a Novel Robotic Finger Concept for Minimal Actuation Variable Impedance Grasping," IEEE Intern. Conf. on Robotics and Automation, pp. 771-776, 2010.